Engineering Structures 319 (2024) 118854

Contents lists available at ScienceDirect

Engineering Structures

journal homepage: www.elsevier.com/locate/engstruct

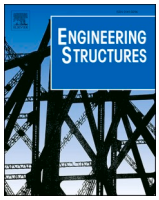

Experimental study of bond-slip relationships in high-performance self-consolidating concrete with plain steel bars

Marcin Dyba *

Chair of Reinforced and Prestressed Concrete Structures, Faculty of Civil Engineering, Cracow University of Technology, Warszawska street 24, Kraków 31–155, Poland

ARTICLE INFO

Keywords:
Adhesion, bond behavior, bond-slip
High-performance concrete
Self-consolidating concrete
Pull-out test

ABSTRACT

Self-consolidating concrete is being used more frequently in structures with high density of reinforcement bars or prestressing strands therefore, it is important to carefully consider whether bond stress-slip relations defined for normal strength concrete can be safely applied to high-strength and self-consolidating concrete. This paper aims to investigate the bond behaviour between plain steel bars and high-performance self-consolidating concrete, with a focus on studying the effect of embedment length and concrete compressive strength on bonding performance. The main parameters that were tested are the active bonded length and the compressive strength of the concrete. The value of adhesive bond stress is discussed, as a factor in determining whether the bar slips against the adhering concrete. Based on the results, it can be observed that the maximum bond stress tends to increase with higher concrete compressive strength, while it decreases with longer embedment length of plain steel bar. Conversely, the adhesive bond tends to increase with longer embedment length and higher concrete compressive strength. The experimental investigations indicate that the bond strength increases proportionally to the square root of the compressive strength of concrete, regardless of the concrete compressive strength. Furthermore, a new bond stress-slip model has been analyzed, which takes into account the initial bond strength (adhesive bond) and the lower convex property to predict the post-peak branch. The model has been compared to the test results, and good agreement has been achieved.

1. Introduction

Since 2000, high-strength concrete structures have often been reinforced with steel of higher tensile strength. Steel with a strength of 700–800 MPa has been used more frequently [1]. Prefabricated units use high-performance concrete, with a compressive strength of 80–120 MPa [2,3], to manufacture pre-tensioned girders. For both applications, it is essential to establish the bond stress-slip relationships between high-strength concrete and reinforcement. In case of structures with high density of reinforcement bars or prestressing strands self-consolidating concrete is used more and more often [4,5]. Self-consolidating high-performance and high-strength concrete is characterized with modified composition of cement concrete in comparison with the same high-strength concrete compacted mechanically [6]. Thus, a question arises whether bond stress-slip relations defined for normal strength concrete can be safely used in case of self-consolidating concrete. The author of this paper is aware that, nowadays, plain bars are no longer used to construct reinforced concrete structures. Consequently, most research of concrete bond phenomenon focuses on elements comprising deformed reinforcement bars. As part of the ongoing research program, it was considered for educational reasons to determine the bond-slip relationships of high-performance concrete (HPC) to plain bars, plain wires, indented wires, and seven-wire strands. The results of experimental studies conducted on mechanically compacted HPC in elements with plain bars and wires are presented in the works [7,8]. The research objective of this paper was to ascertain the impact of the method of placing high-performance self-consolidating concrete on the values of the bond stress and the bond-slip relationship to plain steel bar reinforcement.

Existing calculation models mention adhesion whose overcome conditions bar slip against adhering concrete. However, the value of adhesive stress is not widely discussed. Initial empirical research conducted in the Institute of Building Materials and Structures of the Cracow University of Technology showed that the adhesive bond-stress of high-strength and high-performance concrete to plain steel bars is high and its value depends on concrete compressive strength [7,9].

The mechanism of force transfer between reinforcement and surrounding concrete is different in case of plain steel bars and different in

* Corresponding author.
E-mail address: marcin.dyba@pk.edu.pl.

https://doi.org/10.1016/j.engstruct.2024.118854
Received 11 March 2024; Received in revised form 22 July 2024; Accepted 20 August 2024
Available online 28 August 2024
0141-0296/© 2024 The Author(s). Published by Elsevier Ltd. This is an open access article under the CC BY-NC license (http://creativecommons.org/licenses/by-nc/4.0/).

case of deformed ones. Deformed bars transfer a big part of this force due to the mechanical interlock between surface deformations of bars and surrounding concrete [10–12]. In case of plain bars, force transfer consists in adhesion between concrete and reinforcement, before a given bar slips, and then it occurs as a result of wedging little particles of crumbled concrete, as a result of slipping. It is so-called sliding friction.

2. Review of the state of the art

Abrams [13,14] was one of the first researchers who analyzed the behaviour of bond stress-slip relations. His analyses allowed Abrams to reach the conclusion that bond stress between concrete and plain steel reinforcement bars depends on two main factors: adhesion and slip resistance. Adhesion occurs till the time bar slip takes place, and slip resistance begins when there is relative shift between two materials. Moreover, Abrams stated that maximum bond stress occurs when the slip value is about 0.25 mm and it can be presented as (1).

$$\tau_{b,\max} = 0.19 \bullet f_c \tag{1}$$

Moreover, he put forward relations between maximum bond stress and adhesion $\tau_{b,a}$ (2) and between maximum bond stress and residual bond stress $\tau_{b,f}$ (3). Residual bond stress occurring due to friction (frictional bond stress).

$$\tau_{b,a} = 0.60 \bullet \tau_{b,\max} \tag{2}$$

$$\tau_{b,f} = 0.50 \bullet \tau_{b,\max} \tag{3}$$

Feldman and Bartlett [15,16] conducted their research on bond with the use of the pull-out method, testing 252 specimens with plain bars, with circular and square cross sections. On the basis of the results obtained they proposed empirical expressions serving to calculation the maximum value of bond stress for bars with the diameter of 16 mm and 32 mm, depending on concrete compressive strength, the shape of the cross section of a given reinforcement bars, its roughness and diameter.

According to Model Code 1990 [17], for monotonic loading the value of bond stress τ_b between concrete and reinforcement bars when the specimens are damaged by pulling out or by concrete splitting can be calculated as a function of relative displacement s, parallel to the centreline of a bar according to Eqs. (4–7).

$$\tau_b = \tau_{b,\max} \bullet \left(\frac{s}{s_1}\right)^{\alpha} \quad 0 \le s \le s_1 \tag{4}$$

$$\tau_b = \tau_{b,\max} \quad s_1 < s \le s_2 \tag{5}$$

$$\tau_b = \tau_{b,\max} - \left(\tau_{b,\max} - \tau_{b,f}\right) \bullet \left(\frac{s - s_2}{s_3 - s_2}\right) \quad s_2 < s \le s_3 \tag{6}$$

$$\tau_b = \tau_{b,f} \quad s > s_3 \tag{7}$$

In case of using plain reinforcement bars, the parameters placed in Table 3.1.2. [17] constitute the completion of given relations. It means that $s_1 = s_2 = s_3 = 0.10$ mm, $\alpha = 0.5$,

$\tau_{b,\max} = \tau_{b,f} = 0.30 \bullet \sqrt{f_{ck}}$ for good bond conditions, and

$\tau_{b,\max} = \tau_{b,f} = 0.15 \bullet \sqrt{f_{ck}}$ for all other cases.

In the current version of Model Code 2010 [18], when it comes to plain bars, the only difference is introducing to Table 6.1.2 [18] average compressive strength f_{cm} instead of characteristic compressive strength f_{ck}.

Verderame et al. [19,20], on the basis of the results obtained from their empirical research, suggested the modification of the bond stress-slip model, proposed beforehand by Eligehausen at al. [21] for deformed bars. They introduced the following parameters into the model: $\tau_{b,\max} = 0.31 \bullet \sqrt{f_{ck}}$; $s_{max} = 0.23$ mm, $\alpha = 0.26$, $\tau_{b,f} = 0.43 \bullet \tau_{b,max}$ and $p = 0.06$. Slip s_{max} is defined as the slip value corresponding to maximum bond stress $\tau_{b,max}$, whereas p represent the slope of the softening branch expressed as a function of the secant stiffness ($\tau_{b,max}/s_{max}$). These average values were obtained from research conducted with the help of the pull-out method, on specimens containing reinforcing bars with the diameter of 12 mm, with active length of adhesion equal to 10 times of the bar diameter and average concrete compressive strength (cylindrical samples) equal to 15.9 MPa.

Melo et al. [14] analyzing the results coming from the analysis of 27 specimens with the help of the pull-out method, proposed a new model of bond stress-slip relation which keeps the shape of the ascending curve (up to peak) till reaching the maximum value of bond stress according to the model by Verderame et al. [19,20], but better describes the descending branch expressed by the third-degree polynominal function. The experimental research was performed on specimens made from concrete class C12/15 and C16/20 with bars whose diameters equaled 10, 12 and 16 mm, with the following values of active bonded lengths 5ϕ, 30ϕ and 45ϕ.

In both models (Verderame et. al and Melo at al.) the ascending branch is defined by expressions (4−7), where α is computed in order that the area underneath ($A_{1,mod}$) of the bond-slip curve until s_{max} equals the corresponding area from experimental results. The Verderame et al. [19,20], model for slip value larger than s_{max} is defined by two linear branches, a softening branch (from s_{max} to s_f) followed by a plateau until the ultimate slip (s_u). In the Melo et al. [14] model, after s_{max}, the bond-slip relationship is defined by third-degree polynominal function until the ultimate slip, s_u and is followed by a plateau. A value of 10 mm is assumed for s_u which is based on experimental observations made by Melo et al. [14], and Feldman and Bartlett [15].

The empirical expressions (8−16) were obtained based on statistical analysis of all individual experimental results.

$$\tau_{b,\max} = k \bullet \sqrt{f_c \bullet f_y} \tag{8}$$

$$k = -3.63 \bullet 10^{-5} \bullet \left(\frac{l_{emb}}{\phi}\right)^2 + 1.75 \bullet 10^{-3} \bullet \left(\frac{l_{emb}}{\phi}\right) + 0.0178 \tag{9}$$

$$\tau_{b,f} = 0.41 \bullet \tau_{b,\max} \tag{10}$$

$$\alpha = 1.9 \bullet 10^{-4} \bullet \left(\frac{l_{emb}}{\phi}\right)^2 + 0.088 \tag{11}$$

$$s_{\max} = 9.1 \bullet 10^{-4} \bullet l_{emb} + 0.16 \tag{12}$$

$$p = 2.7 \bullet 10^{-7} \bullet {l_{emb}}^2 - 2.6 \bullet 10^{-5} \bullet l_{emb} + 0.027 \tag{13}$$

$$s_f = \frac{s_{\max} \bullet \left(\tau_{b,\max} + p \bullet \tau_{b,\max} - \tau_{b,f}\right)}{p \bullet \tau_{b,\max}} \tag{14}$$

$$\tau_b = a \bullet s^3 + b \bullet s^2 + c \bullet s + d \tag{15}$$

$$A_{2,\mathrm{mod}} = 5.1 \bullet \tau_{b,\max} + 0.51 \tag{16}$$

Expression (16) was found by fitting a curve to the relationship between the experimental area underneath the bond-slip curve between s_{max} and s_u, and the experimental $\tau_{b,max}$ obtained in all specimen.

In 1997, Magnusson [22] conducted experimental research to compare the behavior of bond stress-slip relations in well-confined high strength concrete and normal strength concrete. Cylindrical specimens with diameters of 300 mm and 350 mm were used, with deformed steel bars of 16 and 20 mm diameter axially embedded. The predicted compressive strength for normal strength concrete was approximately 25 MPa, while for high-strength concrete it was around 100 MPa. Magnusson conducted a series of pull-out tests, which demonstrated that the bond strength (maximum bond stress) increases proportionally with the average compressive strength for both normal and high-strength concrete. The evaluation of bond stress was based on the tests, which involved dividing the tensile force by the interfacial area along the short

embedment length. This was then related to the end slip at the unloaded end. Huang, Engstrom, and Magnusson [23] proposed the following relation (17) based on the results obtained.

$$\tau_{b,\max} = 0.45 \bullet f_{cm} \tag{17}$$

According to the authors, maximum bond stress is achieved with deformed bar slip $s_1 = s_{max} = 0.5$ mm in the case of high-strength concrete. Their proposed model maintains the same relationship as Model Code 1990 for the ascending branch ($\alpha = 0.3$), but introduces modifications to the descending branch to account for the different behavior of high-strength concrete. Additionally, they suggest adopting residual bond stress in the form (18).

$$\tau_{b,f} = 0.40 \bullet \tau_{b,\max} \tag{18}$$

Tests on the bond between high-performance concrete and plain bars were conducted at Cracow University of Technology by Dyba and Seruga [7]. The study investigated the bond performance of mechanically compacted high-performance concrete to 16 mm diameter bars. Pull-out tests were conducted on specimens with a cross-section of 160 × 160 mm and active bond lengths of 2.5, 5, and 7.5 (40, 80, and 120 mm) bar diameters, respectively. The concrete used in the tests had compressive strengths of 40, 60, 72 and 88 MPa. A total of 48 concrete specimens were casted and tested under uniaxial load. The test results indicate that the ratio of maximum bond stress to concrete compressive strength ranges from 0.12 to 0.17. The maximum bond stress increases with an increase in concrete compressive strength and decreases with a longer embedment length of plain steel bars. The adhesive bond stress is approximately 0.55 of the maximum bond stress. Finally, a new bond stress-slip model was proposed, which achieved good agreement between the tests and the theoretical prediction.

Based on the most critical factor for bond strength under a certain bar diameter, which is concrete compressive strength a bond stress-slip model was proposed as follows (19):

$$f_b = \begin{cases} f_{b,a} + (f_{b,\max} - f_{b,a}) \bullet \left(\dfrac{s}{s_{\max}}\right)^{\alpha} & 0 \le s \le s_{\max} \\ f_{b,\max} - a \cdot \ln\left(\dfrac{s}{s_{\max}}\right) & s_{\max} < s < 10mm \end{cases} \tag{19}$$

where: $f_{b,a} = 0.58 \cdot (f_c)^{1/2}$, $f_{b,max} = 1.04 \cdot (f_c)^{1/2}$; concrete compressive strength $f_c = f_{c,cyl}$; slip s, slip at maximum bond $s_{max} = 0.46$ mm; coefficients: $a = 0.85$, $\alpha = 0.35$.

The ascending branch of the model starts from the adhesive bond and represents the contribution of mechanical micro-interlocking and friction on the bond strength. The descending branch represents progressive friction degradation and second-order micro-interlocking. The proposed model formulation is limited to high-performance concrete with a compressive strength range of 40 to 90 MPa.

High-performance concrete is distinguished by its high early strength. Concretes incorporating silica fume and plasticizers display augmented properties. The use of silica fume as a pozzolan appears to be more efficient than the use of fly ash, with the pozzolanic reactions becoming evident at an earlier age than in fly-ash concrete [24]. In examining the impact of silica fume, two factors warrant consideration: the reduction in water demand by the system, which consequently results in a diminished effective water ratio (cement + silica fume), and the pozzolanic reaction of the silica fume. The initial effect results in a reduction in total porosity, while the subsequent effect leads to the refinement of the pore structure without any further reduction in total porosity [24,25].

The objective of the experimental investigation conducted by Gjørv et al. [26] was to examine the impact of silica fume on the mechanical behavior of the steel-concrete bond. Pullout tests were conducted on concrete compressive strength specimens with strengths of 35, 42, 63, and 84 MPa and plain steel bars of 19-mm diameter. The results demonstrated that an increasing addition of silica fume to 16 % by weight of cement resulted in an improvement in pullout strength, particularly in the high-compressive strength range of concrete.

Currently, the work [7] is the only research that considers high-performance concrete bond to plain steel reinforcing bars. There are no public known reports from bond tests on specimens made of self-compacted high-performance concrete. Such a data are crucial for the proper analysis of bond in RC and PC elements made of high-performance self compacted concrete. It is particularly important to define adhesion and its relation to maximum and residual bond stress. It allows specifying or correcting existing calculation models used for both plain and ribbed bars, as well as for strands.

3. Experimental studies

Research pertaining to high-performance self consolidating concrete bond stress to a steel plain bar was performed on concrete designed class of 80/95 after 1, 3, 7 and 28 days of concrete curing. To define the bond stress-slip relations of high-performance concrete and steel plain bars, experimental research was conducted on pull-out specimens measuring 160 × 160 × 160 mm, reinforced with axially embedded plain bars with a diameter of 16 mm. The experimental research program considered the following factors that substantially impact the description of these relations:

- bond embedded length (l_{emb} = 40, 80 and 120 mm),
- and concrete compressive strength (f_c = 41, 55, 68, and 87 MPa),

The program was similar to the one used for bond tests of conventionally compacted high-performance concrete to plain steel bars, described in the paper [7].

3.1. Concrete and concrete mixture

The specimens were casted from a specially prepared cement concrete composition, class C80/95, with ingredients listed in Table 1 per 1 m^3 of concrete. The concrete mixture has been designed to meet all the requirements of self-consolidating concrete [27]. To determine the compressive strength of the concrete and the modulus of elasticity under compression, standard specimens of ϕ150 × 300 mm and 150 × 150 × 150 mm were taken. All the specimens, and standard samples were covered with 3 layers of polyethylene sheet after casting to ensure stable concrete curing conditions [9].

Experimental research was conducted to analyze the mechanical properties of concrete at different stages of curing (1, 3, 7, and 28 days). After being removed from the mold, all specimens and samples for testing were still stored under 3 layers of polyethylene sheet. At each testing stage mechanical properties of concrete were defined. Table 2 contains the results of the mechanical properties of concrete from tests, which were conducted over a period of 90 days. During strength tests, particular samples were measured and weighed, which made it possible to define volumetric concrete density.

Average volumetric density of concrete equals $q = 2539$ kg/m^3 with the coefficient of variation $\nu = 1{,}2$ %.

The consistency of self-consolidating cement concrete composition was defined by three methods [28,29]. Measured average final slump of Abrams come with diameter of ϕ100/200 mm and height of 300 mm was 710 mm, and average final slump of the cone put upside down was

Table 1
High-performance self-consolidating concrete mix composition.

Composition	[kg/m^3]
cement CEM I 42,5 R	475
river sand 0/2 mm	660
basalt aggregate 2/8 mm	616
basalt aggregate 8/16 mm	546
water	168
silica fume (Sika Fume HR-TU)	48
superplasticizer (Sika ViscoCrete 5 −600)	7.8

Table 2
Mechanical properties of HPSCC.

Concrete age	$f_{c,cyl}$ [MPa] (ϕ150 ×300 mm)	$f_{c,cube}$ [MPa] (150 ×150 ×150 mm)	$f_{ct,dir}$ [MPa] (ϕ150 ×300 mm)	E_c [MPa] (ϕ150 ×300 mm)
24 h	41.1	46.9	-	35 840
2 days	51.4	57.4	2.79	38 020
3 days	55.4	65.3	3.06	40 640
7 days	67.7	77.4	4.19	44 370
28 days	87.4	90.2	5.17	47 570
90 days	91.3	94.6	6.37	50 130

680 mm. The dynamics of slump, that is time needed to reach the slump of 500 mm in both cases was high and it equaled T_{500} = (3.0–3.5) s. The measured values correspond to the consistency (fluidity) class SF2 (slump of the range 660 – 760 mm). Class SF2 is appropriate for typical use – walls, columns, floors and beams. Additionally, average final cone of spreading of cone with diameter of ϕ130/200 mm and height 200 mm was defined and it was 520 mm (Fig. 1). The used cement concrete composite met all criteria for self-consolidating cement concrete composites: the criteria of fluidity, workability and resistance to segregation. While putting concrete in its moulds for concrete testing there was not report of aggregate falling in the samples. The thickness of mortar (without coarse aggregate) on top of the samples did not exceed 7 mm in any measured element. It was proven by observed plane of shearing after tensile strength tests by sample splitting (cubic samples with 150 mm sides).

3.2. Steel plain bars

St3Sx-b steel reinforcement bars with a diameter of 16 mm were utilized in the study. Steel strength tests were conducted using the Zwick-Roell Z1200 machine, which automatically measures tensile strength through an in-built force gauge. Displacement and strains were recorded by an incremental extensometer synchronized with the machine software.

The extensometer's measuring base was 180 mm. Load steering was performed at a speed of 20 MPa/s until the yield point was reached. After that, it was automatically switched to displacement control at a speed of 0.003 1/s within the flow range. The experimental research was conducted on 9 bars. The test procedure is shown in Fig. 2, and Table 3 presents the average values of the tested mechanical properties of the reinforcing steel.

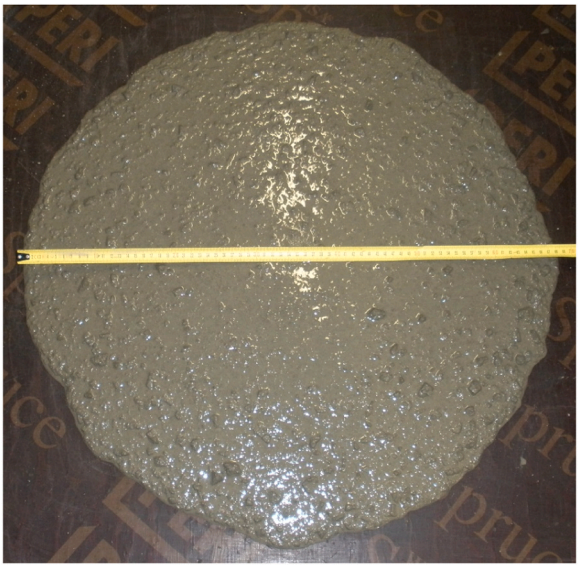

Fig. 1. Self-consolidating mixture slump flow test.

3.3. Pull-out specimens

Based on performed studies for mechanically compacted high-performance concrete [7], as well as taking into account research results obtained in various scientific centres [14, 15, 16, 19, 20, 26], it was decided to adopt 3 active bond lengths equalling 2.5, 5, and 7.5 bar diameter for experimental tests (40, 80, and 120 mm). These lengths can be achieved by using a module mould that equips bars with protective PVC tubes measuring 120, 80, and 40 mm long (as shown in Fig. 3). To prevent cement paste leakage, the free space between the bar and its PVC tube, as well as between the PVC tube and the front side of the mould, was filled with silicon.

Two series of specimens (labelled I and II) were prepared, each with 24 specimens (8 for each embedment length). Four specimens, two from series I and two from series II, with the same active bond length were tested and analyzed at each stage (1, 3, 7, and 28 days of concrete curing).

3.4. Pull-out test procedure

In order to assess the concrete-steel bond-slip, a pullout test method was employed, based on based on direct pullout test [30–34]. The test method developed at the Institute for Building Materials and Structures of the Cracow University of Technology [9, 35–37] utilises a separate measuring system from the pullout mechanism, enabling the precise measurement of relative displacement of materials. Furthermore, it accurately reproduces both the adhesion and frictional forces, as well as the mechanical interlock effects.

The specimens for testing the bond stress-slip relation with axially embedded steel reinforcing bars were placed in a specially designed and constructed three-dimensional steel frame (see Fig. 4). The structure comprises two rigid steel plates, an upper one and a bottom one, joined by four steel hangers made of steel bars with a hexagonal cross-section. The frame structure is attached to the strength measuring machine via a hinge using a steel joint made of high-strength steel screwed to the upper steel plate of the frame. The bottom steel plate has a centrally drilled hole through which a bar from the concrete specimen can be inserted. To ensure a better fit between the concrete specimen and the steel plate, a hard fiberboard is placed between them. The Zwick-Roell Z1200 testing machine grips a longer and lower bar section. The plain bar was subjected to a jaw pressure of 250 bar. The frame structure is lifted by the force from the steering mechanism, which transfers the load on the concrete specimen by exerting pressure on the bottom surface. Placing the reinforcement in the gripping jaws of the testing machine prevented it from moving along with the concrete specimen, causing the plain bar to slip toward the concrete. Load steering was controlled by displacement at a rate of 0.01 mm/s, which is recommended for high-strength concrete elements. The force value was continuously and automatically registered by the recording system. The initial force value was 1 kN. The study measured the relative displacement for a given force using a system of two arms of the incremental extensometer. The upper arms recorded the displacement of a steel plain bar, while the lower arms recorded the displacement of aluminium angles that were glued to the concrete surface, relative to their original location. The spacing of the aluminium angles was 50 mm, and the extensometer's arm spacing

Fig. 2. Tension test procedure for plain steel bars ϕ16 mm: a) measurement, b) broken bar.

Table 3
Mechanical properties of reinforcing steel.

cross-section area A_s [mm^2]	tensile strength f_u [MPa]	high yield point R_{eH} [MPa]	high yield point R_{eH} [MPa]	modulus of elasticity E_s [MPa]	elongation of measuring base A_{180} [%]
201	465	318	304	207,260	29.65

was 40 mm. The extensometer reading was accurate to within 0.12 μm. The research was conducted until the displacement value of 10 mm was reached, to observe changes in pull-out force to slip after the loss of adherence.

4. Test results and analysis of the results

The failure mode was the same for all the test pull-out elements. There was a slip of the bar at the free end, which gradually increased with the pull-out force. Splitting cracks did not occur along the centre-line of the bar in any specimen. After performing the tests, certain test elements were split along the axis of the reinforcement. Fig. 5 shows an example of such a specimen.

Fig. 6a, 6b, 6c, and 6d present the results of experimental research on the pullout force-slip relationships for specimens with an embedment length of 40, 80, and 120 mm. The specimens were made of self-compacted high-performance concrete with compressive strengths of 41, 55, 68, and 87 MPa.

$$f_b = \frac{F}{\phi \bullet \pi \bullet l_{emb}} \tag{20}$$

where F is pullout force measured during the test, ϕ is the bar diameter and l_{emb} us the embedded bar length.

To analyze the results obtained, bond stress for a slip value of 10 was calculated for each specimen, taking into account dependency from Eq. 20. The results for concrete compressive strengths of 41, 55, 68, and 87 MPa are displayed in Tables 4–7. The tables also include the maximum values of bond stress and corresponding slip values, as well as the bond stress values where adhesion loss was registered. In addition, the tables present the calculated average bond stress values, standard deviations, and coefficients of variation.

Based on the presented results, an average bond stress-slip relation

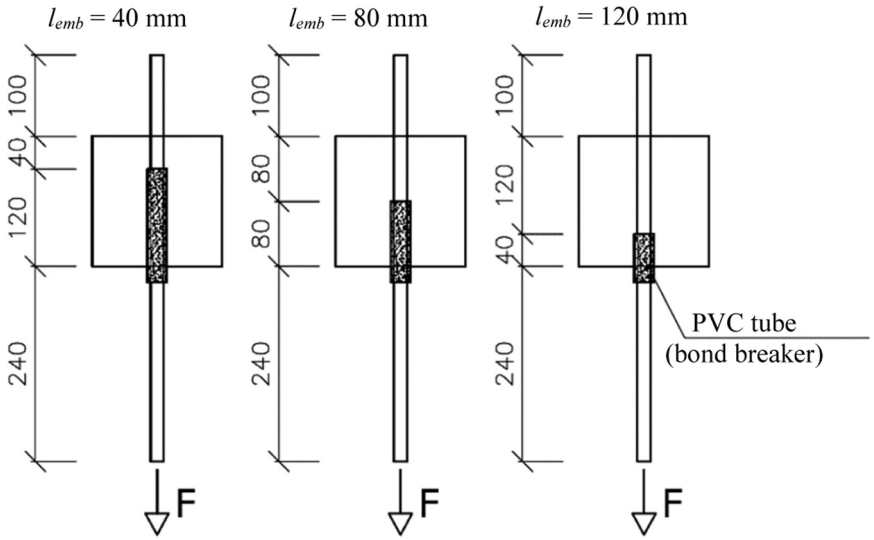

Fig. 3. Test specimens with different active bond embedded lengths geometry [mm].

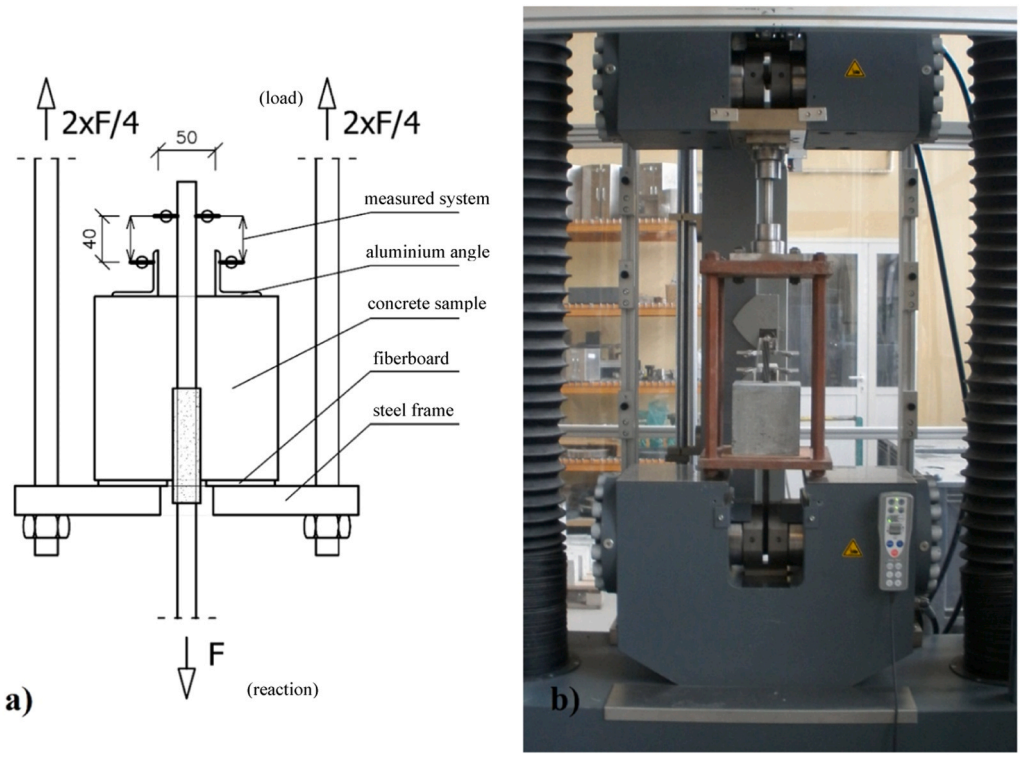

Fig. 4. General view of testing setup: a) scheme (dimensions in mm), b) real setup.

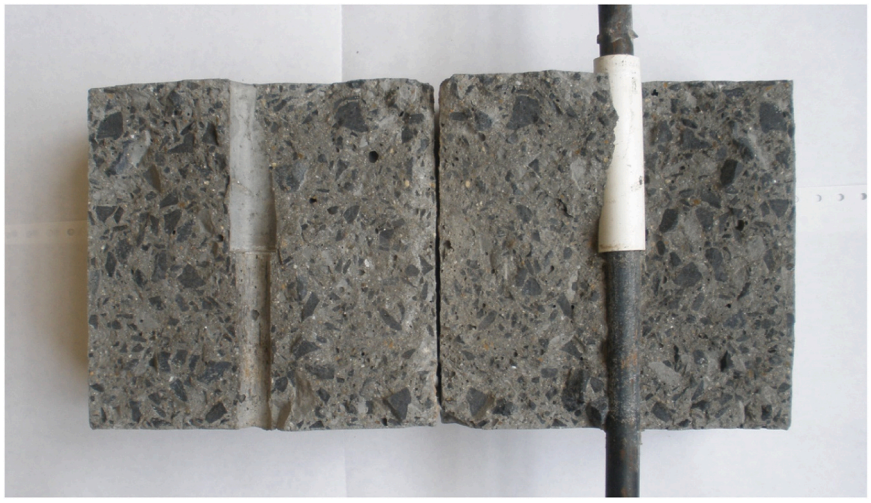

Fig. 5. Specimen after splitting cut along reinforcement bar.

was calculated for each analyzed active bonded length of a plain 16 mm diameter bar, depending on the compressive strength of the concrete. Figs. 7, 8, and 9 show the obtained bond stress-slip relations. The bond stress of HPSCC increases with the increase in concrete compressive strength for each analyzed active bonded length of the plain bar.

Fig. 10a, 10b, 10c, and 10d show the distribution of average bond stress-slip relations for three analyzed active bonded lengths, calculated for concrete compressive strengths of 41, 55, 68, and 87 MPa, respectively. The maximum bond stress was obtained for an active bonded length of 40 mm in the case of concrete compressive strengths of 55, 68, and 87 MPa.

Fig. 11 shows the distribution of average bond stress in the slip function for a given concrete compressive strength, taking into account the analyzed active bonded bar lengths. The falling branch of the chart descends regularly after reaching the maximum bond stress for each analyzed concrete compressive strength value.

Table 8 summarizes the average values of the adhesive bond, maximum values of bond stress, and average values of bar slip corresponding to the last one. Additionally, it includes the average values of residual bond stress for a slip value of $s = 10$ mm. These values were obtained for four analyzed concrete compressive strength values and three active bonded lengths. In addition, the text presents a comparison between the calculated values of adhesive bond, maximum bond stress, and residual bond stress to the average concrete compressive strength. The ratios of adhesive bond and residual bond stress to the maximum bond stress, as well as the ratio of residual bond stress to adhesive bond, are also included.

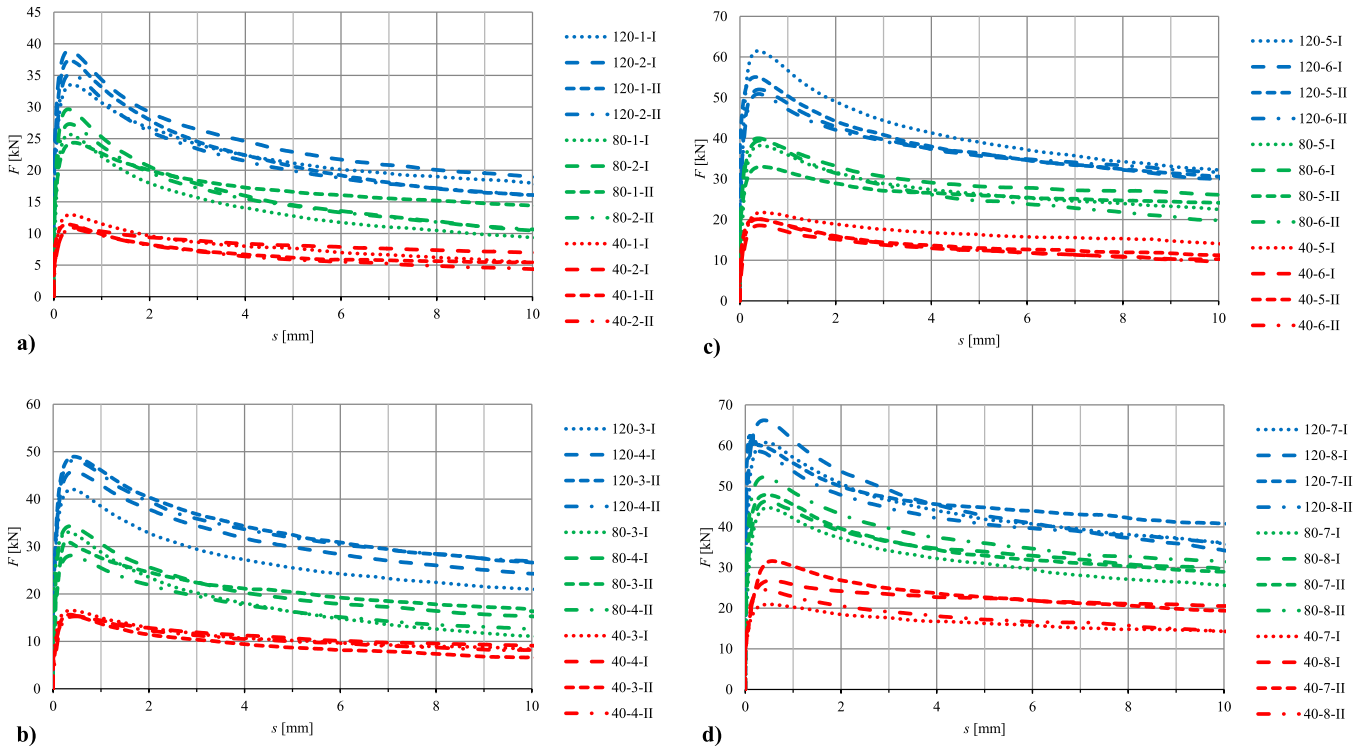

Fig. 6. Tensile force-slip relationship of a plain steel bar of 16 mm dia. with effective bonded length of 40, 80 and 120 mm, in specimens of HPSCC: a) $f_c = 41$ MPa, b) $f_c = 55$ MPa, c) $f_c = 68$ MPa, d) $f_c = 87$ MPa.

Table 4
Bond strength of HPSCC to plain steel bars 16 mm dia. tested on specimens of concrete compressive strength of 41 MPa.

***s* [mm]**	f_b (l_{emb} = 40 mm) [MPa]				f_b (l_{emb} = 80 mm) [MPa]				f_b (l_{emb} = 120 mm) [MPa]				***Distribution parameters***	
	2-II	**1-II**	**2-I**	**1-I**	**2-II**	**1-II**	**2-I**	**1-I**	**2-II**	**1-II**	**2-I**	**1-I**	$f_{b,ave}$ **[MPa]**	***CoV*** **[MPa]**
adhesion	1.75	2.78	2.25	1.21	3.11	3.07	2.07	1.77	2.50	3.09	3.07	2.44	**2.43**	**26.07**
0.01	2.05	3.70	2.40	1.54	3.31	3.47	2.45	2.03	2.64	3.32	3.48	2.69	**2.76**	**25.19**
0.025	2.56	4.05	2.82	2.49	3.92	3.67	3.72	3.48	3.22	3.88	4.18	3.18	**3.43**	**16.82**
0.1	4.11	5.13	4.13	5.15	5.67	5.02	6.32	5.20	4.86	5.30	5.69	4.65	**5.10**	**12.39**
0.254	5.19	5.69	5.23	6.36	6.73	5.92	7.34	6.33	5.77	6.14	6.42	5.47	**6.05**	**10.48**
1	4.81	4.93	5.14	5.73	5.93	5.64	6.28	5.52	5.19	5.49	5.69	5.09	**5.45**	**7.97**
2.54	3.77	3.84	4.61	4.48	4.51	4.73	4.71	4.30	4.07	4.30	4.56	4.19	**4.34**	**7.38**
4	3.17	3.32	4.17	3.97	3.85	4.30	3.97	3.50	3.55	3.71	4.08	3.71	**3.78**	**9.13**
6	2.75	2.92	3.91	3.48	3.31	4.00	3.37	2.92	3.11	3.18	3.60	3.34	**3.32**	**11.56**
8	2.43	2.80	3.66	3.10	2.94	3.78	2.97	2.61	2.85	2.83	3.33	3.15	**3.04**	**13.13**
10	2.17	2.70	3.48	2.70	2.65	3.59	2.60	2.33	2.65	2.67	3.15	2.98	**2.81**	**15.05**
$f_{b,max}$ **[MPa]**	5.35	5.70	5.43	6.45	6.80	6.06	7.38	6.38	5.85	6.20	6.46	5.56	**6.13**	**9.81**
$s(f_{b,max})$ **[mm]**	0.39	0.29	0.44	0.35	0.34	0.42	0.31	0.33	0.35	0.34	0.32	0.38	**0.35**	**12.55**

Table 5
Bond strength of HPSCC to plain steel bars 16 mm dia. tested on specimens of concrete compressive strength of 55 MPa.

***s* [mm]**	f_b (l_{emb} = 40 mm) [MPa]				f_b (l_{emb} = 80 mm) [MPa]				f_b (l_{emb} = 120 mm) [MPa]				***Distribution parameters***	
	4-II	**3-II**	**4-I**	**3-I**	**4-II**	**3-II**	**4-I**	**3-I**	**4-II**	**3-II**	**4-I**	**3-I**	$f_{b,ave}$ **[MPa]**	***CoV*** **[MPa]**
adhesion	2.36	2.65	3.03	2.38	3.06	2.93	2.47	3.81	3.25	3.40	2.88	3.10	**2.94**	**14.76**
0.01	2.36	2.65	3.42	2.87	3.08	3.04	2.86	4.82	3.27	3.46	3.21	3.40	**3.20**	**18.95**
0.025	2.52	3.29	3.89	3.67	3.76	3.38	4.07	5.53	3.92	4.14	4.00	3.84	**3.83**	**18.18**
0.1	5.20	5.97	5.91	6.74	5.77	5.52	7.07	7.37	6.23	6.54	6.08	5.77	**6.18**	**10.36**
0.254	7.31	7.65	7.33	8.08	6.86	7.69	8.42	8.18	7.74	7.89	7.39	6.84	**7.62**	**6.48**
1	7.10	6.82	7.17	7.45	6.34	6.86	7.62	7.17	7.51	7.64	7.12	6.38	**7.10**	**6.14**
2.54	5.82	5.37	6.10	6.03	5.27	5.81	5.94	5.34	6.17	6.36	5.93	5.13	**5.77**	**6.92**
4	5.22	4.68	5.60	5.31	4.40	5.25	5.04	4.48	5.58	5.69	5.26	4.51	**5.08**	**9.03**
6	4.78	4.06	5.03	4.80	3.76	4.78	4.45	3.68	5.05	5.12	4.70	4.02	**4.52**	**11.36**
8	4.32	3.66	4.74	4.44	3.36	4.43	4.08	3.13	4.72	4.70	4.32	3.72	**4.14**	**13.20**
10	4.06	3.29	4.53	4.15	3.14	4.07	3.80	2.76	4.46	4.42	4.03	3.48	**3.85**	**14.69**
$f_{b,max}$ **[MPa]**	7.65	7.78	7.60	8.21	6.99	7.70	8.53	8.21	7.99	8.12	7.61	6.97	**7.78**	**6.07**
$s(f_{b,max})$ **[mm]**	0.45	0.36	0.47	0.40	0.40	0.27	0.36	0.32	0.44	0.43	0.44	0.40	**0.39**	**15.29**

Table 6
Bond strength of HPSCC to plain steel bars 16 mm dia. tested on specimens of concrete compressive strength of 68 MPa.

s [mm]	f_b (l_{emb} = 40 mm) [MPa]				f_b (l_{emb} = 80 mm) [MPa]				f_b (l_{emb} = 120 mm) [MPa]				*Distribution parameters*	
	6-II	5-II	6-I	5-I	6-II	5-II	6-I	5-I	6-II	5-II	6-I	5-I	$f_{b,ave}$ [MPa]	*CoV* [MPa]
adhesion	3.23	4.64	2.11	3.76	4.22	4.82	4.42	3.23	3.51	6.54	3.60	3.66	**3.98**	**27.39**
0.01	3.72	5.10	2.34	4.25	4.28	4.95	4.77	3.28	3.86	6.68	3.64	3.78	**4.22**	**25.75**
0.025	5.47	6.02	3.25	4.61	5.41	5.32	5.68	5.12	4.54	7.17	4.66	5.31	**5.21**	**18.14**
0.1	7.65	8.63	6.64	7.49	8.35	6.85	8.00	6.89	6.88	8.47	7.19	7.99	**7.59**	**9.22**
0.254	9.79	9.98	8.93	10.28	9.78	7.99	9.54	9.21	8.28	9.10	8.45	10.03	**9.28**	**8.05**
1	9.16	9.23	8.44	10.37	9.13	7.89	9.27	8.93	7.80	8.36	8.05	9.40	**8.84**	**8.48**
2.54	7.42	7.49	7.13	9.02	7.38	6.92	7.84	7.46	6.71	6.99	6.80	7.68	**7.40**	**8.36**
4	6.53	6.79	6.45	8.34	6.50	6.61	7.24	6.81	6.20	6.30	6.19	6.85	**6.73**	**8.74**
6	5.88	6.29	5.89	7.84	5.93	6.33	6.92	6.29	5.78	5.74	5.75	6.16	**6.23**	**9.77**
8	5.38	5.95	5.44	7.62	5.42	6.14	6.73	5.96	5.52	5.37	5.34	5.68	**5.88**	**11.67**
10	4.80	5.59	5.10	7.00	4.94	6.01	6.49	5.59	5.26	5.07	4.96	5.34	**5.51**	**12.25**
$f_{b,max}$ [MPa]	10.00	10.07	9.24	10.83	9.95	8.21	9.81	9.51	8.44	9.13	8.63	10.20	**9.50**	**8.32**
$s(f_{b,max})$ [mm]	0.38	0.33	0.40	0.44	0.39	0.44	0.43	0.42	0.39	0.33	0.40	0.40	**0.40**	**9.15**

Table 7
Bond strength of HPSCC to plain steel bars 16 mm dia. tested on specimens of concrete compressive strength of 87 MPa.

s [mm]	f_b (l_{emb} = 40 mm) [MPa]				f_b (l_{emb} = 80 mm) [MPa]				f_b (l_{emb} = 120 mm) [MPa]				*Distribution parameters*	
	8-II	7-II	8-I	7-I	8-II	7-II	8-I	7-I	8-II	7-II	8-I	7-I	$f_{b,ave}$ [MPa]	*CoV* [MPa]
adhesion	5.07	5.28	5.46	4.08	6.31	6.11	4.57	4.42	6.68	5.35	6.24	5.49	**5.42**	**14.93**
0.01	5.32	5.35	6.07	4.73	6.92	6.14	4.68	4.50	7.15	6.76	6.53	5.89	**5.84**	**15.72**
0.025	6.43	5.87	6.74	5.68	8.01	7.18	7.13	6.39	7.94	9.02	7.32	7.41	**7.09**	**13.44**
0.1	9.95	8.99	9.39	8.33	11.08	9.96	8.99	8.18	9.87	10.35	9.60	8.68	**9.45**	**9.05**
0.254	11.88	13.23	12.42	10.02	12.78	11.62	11.10	10.59	9.73	10.00	10.83	9.88	**11.17**	**10.79**
1	11.35	15.08	12.85	10.07	12.08	11.31	10.94	10.47	8.90	9.24	10.19	9.47	**11.00**	**15.79**
2.54	9.80	12.79	11.82	8.93	10.20	9.42	9.32	8.81	7.62	8.00	8.49	7.97	**9.43**	**16.51**
4	8.99	11.78	11.29	8.33	9.30	8.56	8.63	8.02	7.00	7.55	7.53	7.30	**8.69**	**17.28**
6	8.27	10.91	10.86	7.83	8.62	7.92	8.19	7.35	6.58	7.28	6.77	6.75	**8.11**	**17.85**
8	7.84	10.28	10.50	7.38	8.14	7.54	7.67	6.75	6.28	7.00	6.18	6.32	**7.66**	**18.66**
10	7.12	9.65	10.22	7.12	7.82	7.20	7.35	6.37	6.00	6.77	5.67	5.94	**7.27**	**19.32**
$f_{b,max}$ [MPa]	12.20	15.72	13.32	10.42	13.00	11.92	11.52	11.13	10.12	10.35	10.99	10.08	**11.73**	**14.13**
$s(f_{b,max})$ [mm]	0.41	0.56	0.53	0.48	0.40	0.45	0.46	0.49	0.36	0.40	0.39	0.45	**0.45**	**13.32**

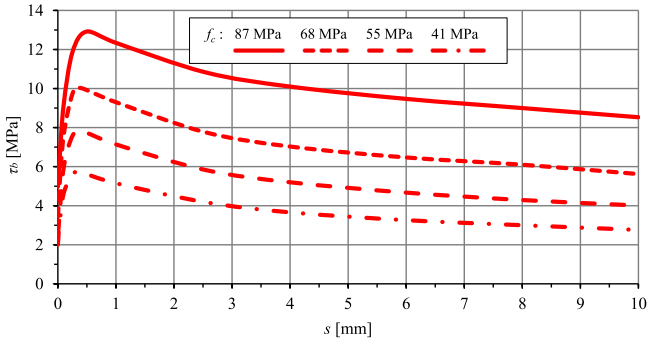

Fig. 7. Average values of bond stress-slip relationship in HPSCC specimen with plain steel bar (l_{emb} = 40 mm).

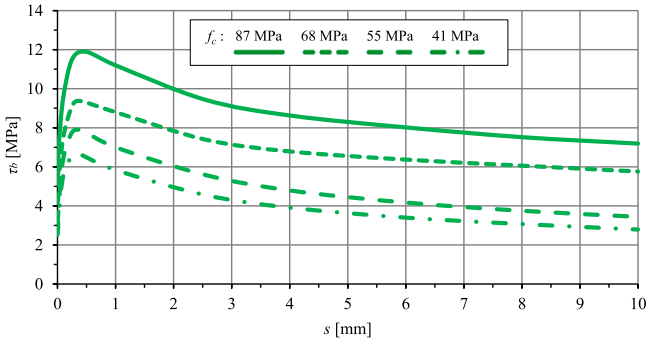

Fig. 8. Average values of bond stress-slip relationship in HPSCC specimen with plain steel bar (l_{emb} = 80 mm).

5. Discussion of the results and bond-slip models considerations

To assess the suitability of the calculation bond models for concrete and plain bars as described in MC 1990 [17], MC2010 [18], *fip* bulletin 10 [30], and recent scientific papers [14, 19, 20] to apply them to plain hot-rolled bars embedded in high-performance concretes, a research study was conducted to determine the characteristic slip values and corresponding bond stresses. According to the experimental study and analysis, there appear to be notable differences between the bond stress-slip relationships for high-performance concrete and the models proposed for normal-strength concrete. This conclusion is supported by the bond distribution shape shown in Fig. 11, the numerical values, and the calculated coefficients in Table 9. It is recommended that these findings be considered when evaluating the performance of concrete in various applications.

First of all, the slippage value s_1 (slip at the maximum value of bond stress) changes significantly, and must be distinguished from s_2 (slip for the start point of the descending branch of bond stress chart) and s_3 (slip for residual bond stress) slippages. Secondly, the adhesive bond has to be considered a non-zero value.

For specimens made of HPSCC, the average value from tests is 0.40 mm, which is comparable to the value of 0.50 mm proposed by Huang, Engstrom, and Magnusson [23] in their simplified model for high-strength concrete, and 0.46 mm proposed by Dyba and Seruga [7] for high-performance mechanically compacted concrete.

Other important parameters, calculated as average values for four analyzed concrete compressive strength values (41, 55, 68, and 87 MPa) are as follows:

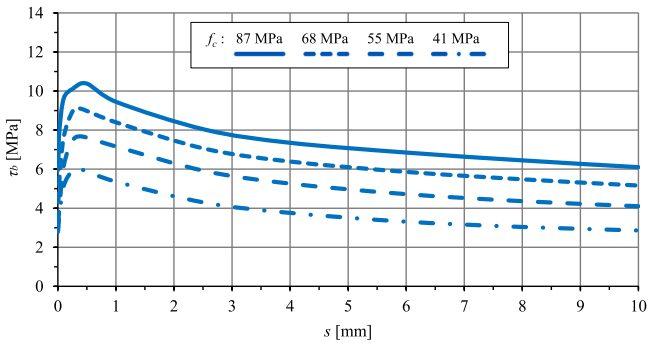

Fig. 9. Average values of bond stress-slip relationship in HPSCC specimen with plain steel bar (l_{emb} = 120 mm).

- average adhesive stress $f_{b,a} = 0.058 \cdot f_{cm} = 0.41 \cdot f_{b,max}$,
- average maximum bond stress $f_{b,max} = 0.14 \cdot f_{cm}$,
- average residual bond stress $f_{b,res} = 0.54 \cdot f_{b,max} = 0.076 \cdot f_{cm}$.

Bond parameters calculated as a function of concrete compressive strength are comparable to those proposed by Abrams [13,15]. However, it should be noted that the coefficients are consistently lower, as they apply to high-strength concrete, not ordinary concrete.

A better match is observed for the coefficients proposed by contemporary researchers [7, 14, 19, 20] in reference to tests performed on high-strength concretes. The bond-slip function models proposed by Melo et al. [14], as well as Verderame et al. [19,20], although graphically represented by simple functions, are nevertheless too computationally complex for practical applications. The model proposed by Dyba and Seruga [7] for high-strength concretes also describes well the development of bond stress in self-compacting concretes as a function of slip. In order to accurately represent the bond stress-slip model [7] for the tested HSSCC concrete and plain bars, the average parameters of function (19) $f_{b,a}$ = 3.69 MPa, $f_{b,max}$ = 8.79 MPa, and s_{max} = 0.4 mm, were derived from the tests, while the coefficients a and α were modified (a = 1.25, α = 0.35). Fig. 12 illustrates the superimposed plots of the average values of the bond-slip relationship for average strength of HPSCC (f_c = 62.8 MPa) and plain steel bar from tests and the model considerations. The results demonstrate a high degree of agreement. This model is straightforward and suitable for engineering applications, as it does not require advanced calculations. In the case of the absence of experimental data for HSSCC and plain steel bar, it is recommended that the following function parameters be adopted: $f_{b,a} = 0.46 \cdot (f_c)^{1/2}$, $f_{b,max} = 1.11 \cdot (f_c)^{1/2}$; concrete compressive strength $f_c = f_{c,cyl}$; slip at maximum bond s_{max} = 0.40 mm; coefficients: a = 1.25, α = 0.35. In contrast, the models described in MC1990 and MC2010 exhibited relatively poorly in terms of test results. Although computationally simplest, these models completely fail to reflect the development of the phenomenon and bond stress as the plain bar progresses through the concrete [30].

The slip value s_1 was experimentally proven to substantially increase due to high adhesion, ranging from 2.3 to 5.4 MPa, and sufficiently high maximum bond stress, ranging from 6.1 to 11.7 MPa. It is worth noting that the post-critical curve of bond stress-slip relations falls gently after

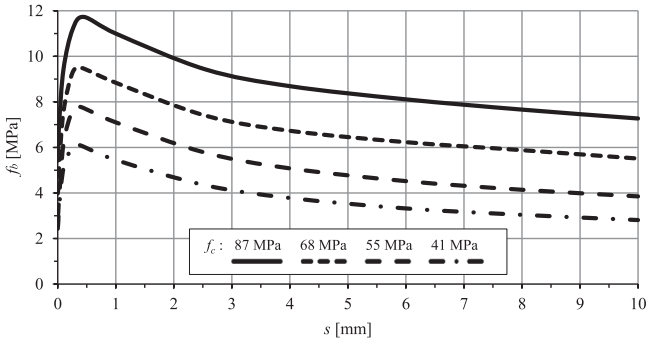

Fig. 11. Average values of bond stress-slip relationship for HPSCC to plain steel bar taking into consideration all tested specimens.

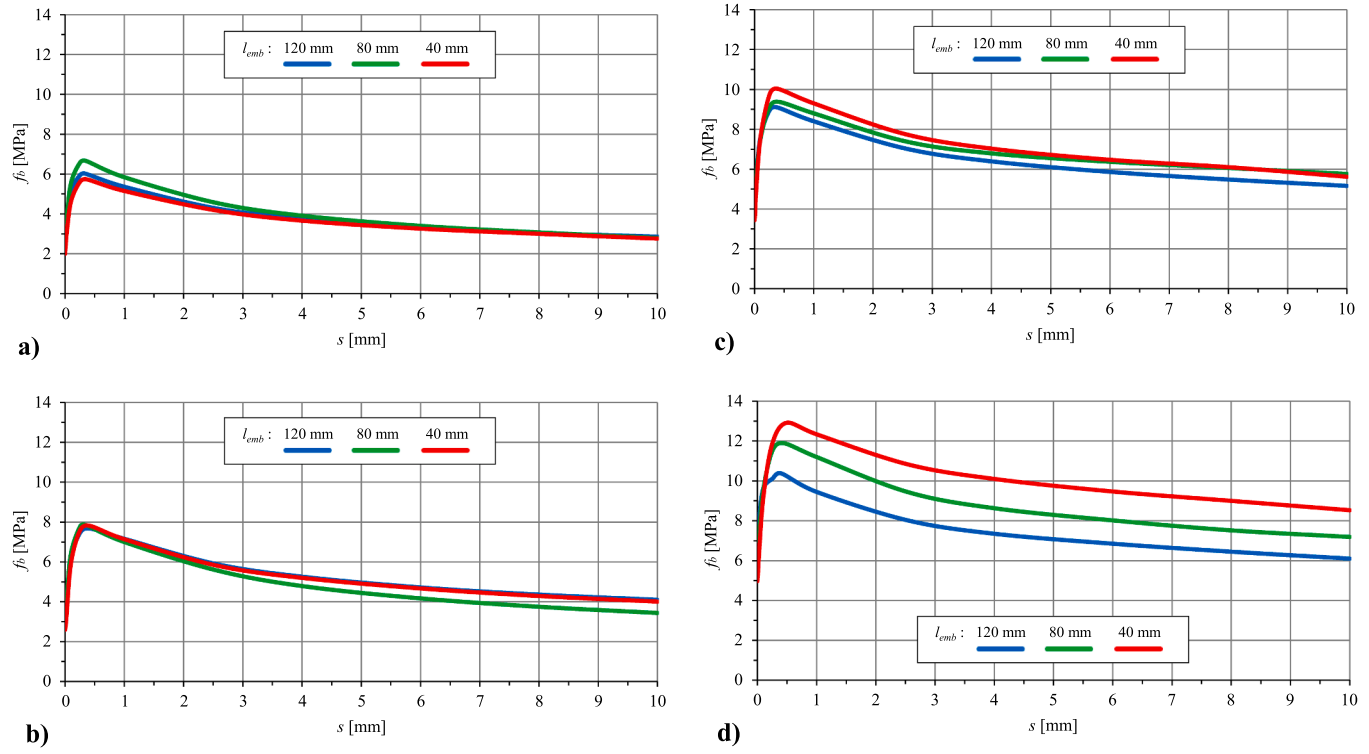

Fig. 10. Average values of bond stress-slip relationship for HPSCC to plain steel bar with varied effective bonded length: a) f_c = 41 MPa, b) f_c = 55 MPa, c) f_c = 68 MPa, d) f_c = 87 MPa.

Table 8
Average values of HPSCC bond strength to a plain steel bar 16 mm dia.

f_c [MPa]	f_{ba} [MPa]	$f_{b,max}$ [MPa]	$f_{b,res}$ [MPa]	s_{max} [mm]	$f_{b,a}/f_{cm}$	$f_{b,max}/f_{cm}$	$f_{b,res}/f_{cm}$	$f_{b,a}/f_{b,max}$	$f_{b,res}/f_{b,max}$	$f_{b,res}/f_{b,a}$
41	2.34	6.13	2.81	0.35	0.059	0.150	0.069	0.396	0.458	1.156
55	2.94	7.78	3.85	0.39	0.053	0.141	0.070	0.378	0.495	1.310
68	3.98	9.50	5.51	0.40	0.059	0.140	0.081	0.419	0.580	1.384
87	5.42	11.73	7.27	0.45	0.062	0.135	0.084	0.462	0.620	1.341
average	-	-	-	0.40	0.058	0.141	0.076	0.414	0.538	1.298

Table 9
Influence of the HPSCC compressive strength and the square root of the strength on the relative bond stress-slip relationship for a plain steel bar 16 mm dia.

s [mm]	f_b/f_c					***CoV*** [%]	$f_b/(f_c)^{½}$					***CoV*** [%]
	41	**55**	**68**	**87**	**average**		**41**	**11**	**68**	**87**	**average**	
adhesion	0.059	0.053	0.059	0.062	0.058	6.29	0.380	0.396	0.483	0.581	0.460	20.12
0.01	0.067	0.058	0.062	0.067	0.064	6.90	0.431	0.431	0.512	0.626	0.500	18.43
0.025	0.084	0.070	0.077	0.081	0.078	7.99	0.536	0.516	0.632	0.760	0.611	18.25
0.1	0.124	0.112	0.112	0.109	0.114	6.09	0.796	0.833	0.920	1.013	0.891	10.85
0.254	0.148	0.139	0.136	0.128	0.138	5.72	0.945	1.027	1.125	1.198	1.074	10.31
1	0.133	0.129	0.130	0.126	0.130	2.07	0.851	0.957	1.072	1.179	1.015	13.98
2.54	0.106	0.105	0.109	0.108	0.107	1.79	0.678	0.778	0.897	1.011	0.841	17.19
4	0.092	0.092	0.099	0.100	0.096	4.32	0.590	0.685	0.816	0.932	0.756	19.77
6	0.081	0.082	0.092	0.093	0.087	7.25	0.518	0.609	0.755	0.869	0.688	22.57
8	0.074	0.075	0.086	0.088	0.081	9.00	0.475	0.558	0.713	0.821	0.642	24.16
10	0.069	0.070	0.081	0.084	0.076	10.05	0.439	0.519	0.668	0.779	0.601	25.28

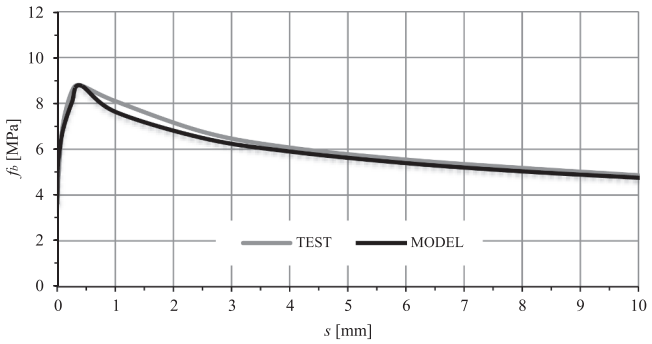

Fig. 12. Bond stress-slip relationship from tests and model considerations.

reaching $f_{b,max}$, as evidenced by the value of $f_{b,res} = 0.54 \cdot f_{b,max}$ for $s = 10$ mm. This value significantly exceeds the adhesive bond ($1.3 \cdot f_{b,a}$).

In the case of high-performance concrete, there is a significant adhesive bond. The adopted test method allows for the evaluation of the real adhesive bond. It is important to note that slip values were measured at the free end of the steel plain bar. Therefore, it can be concluded that the proposed relation (4) [14, 17–20] for the ascending branch (based on the results obtained from the pull-out test method) may not be reliable for high-performance concrete. The initial bond strength $f_{b,a}$ (adhesive bond) depends on two factors: concrete compressive strength and embedment length. Tables 4 to 7 show that chemical adhesion increases with bonding area, which is larger in specimens with longer embedment lengths. The adhesion bond increases with an increase in concrete strength. Of course, these are, not the only factors influencing adhesion, but those which have been tested.

The length of embedment and concrete strength also affect the bond after losing adhesion. The decrease in maximum bond stress with larger embedment length is observed in the tables mentioned above, as well as in Fig. 10c, and 10d. The maximum value of the bond stress-slip relation is achieved for an embedment length of 40 mm for concrete strengths of 87 and 68 MPa. For a concrete strength of 41 MPa, the maximum value of the bond stress-slip relation is achieved with an embedment length of 80 mm. Other researchers [38–40], have also reported a decrease in ultimate bond strength with larger embedment lengths. This is mainly due to the non-linear distribution of bond stress, which is carried by friction and mechanical locking action along the embedment length. This distribution becomes increasingly non-uniform as the embedment length increases.

The study examined the dependency of the relative bond stress f_b/f_{cm} and $f_b/(f_{cm})^{½}$ on the results of the bond stress-slip relationship obtained for specimens with embedded lengths of 40, 80, and 120 mm, for the analyzed concrete compressive strength. Table 9 presents the influence of HPSCC compressive strength and the square root of the strength on the relative bond stress-slip relationship for 16 mm diameter steel plain bar. It can be concluded that the maximum bond strength increases proportionally to the square root of the compressive strength of concrete.

6. Conclusions

The experimental program aimed to investigate the bond behavior between steel plain bars and high-performance self-consolidating concrete, with a focus on studying the effect of embedment length and concrete compressive strength on bonding performance. The main parameters that were tested are the active bonded length and the compressive strength of the concrete. After conducting an experimental study and analysis on the bond between high-performance self-consolidating concrete and steel plain bar, the following conclusions were reached:

- It has been observed that the bond stress-slip relationship remains stable for concrete compressive strength ranging from 40 to 90 MPa. The maximum bond stress value, $f_{b,max} = 0.14 \cdot f_{cm}$, is predicted to occur at a bar slip of 0.4 mm. The residual bond stress, $f_{b,res} = 0.08 \cdot f_{cm}$, is predicted for a bar slip of 10 mm.
- When considering the bond phenomenon to plain steel bars in high-performance concrete, particularly self-consolidating concrete, it is crucial to acknowledge the significant adhesive bond that exists and cannot be disregarded. This bond is a fundamental aspect of the concrete bond behavior and must be taken into account in an analysis of bond stress development. The initial bond strength (adhesive bond) increases with longer embedment length and higher compressive concrete strength. In practical application, the relationship $f_{b,a} = 0.06 \cdot f_{cm}$ may be adopted in the case of high-performance self-consolidating concrete.

- The maximum bond stress decreases with the longer embedment length of the steel plain bar. The experimental investigations demonstrated that the maximum bond strength increases proportionally to the square root of the compressive strength of concrete independently of the concrete compressive strength.
- An analysis of the compatibility of the test results with known models of the bond stress-slip relationship was performed. The model described in the MC1990 and MC2010 standards cannot be applied to consider the adhesion of bars embedded in high-performance concrete, including self-compacting ones. A good representation of the phenomenon could be obtained for the Melo et al. [14], Verderame et al. [19,20], and Dyba and Seruga [7] models (Fig. 12). For practical purposes, it is recommended to use the Dyba and Seruga model. The relevant parameters of the function can be found in Section 5 of the paper.

Author-statement

I hereby declare that I am the sole author of the paper „Experimental study of bond-slip. relationships in high-performance self-consolidating concrete with plain steel bars ” and that I have. not used any sources other than those listed in the bibliography and identified as references. I. further declare that I have not submitied this paper at any other publisher and institution.

CRediT authorship contribution statement

Marcin Dyba: Writing – review & editing, Writing – original draft, Visualization, Validation, Supervision, Software, Resources, Project administration, Methodology, Investigation, Funding acquisition, Formal analysis, Data curation, Conceptualization.

Declaration of Competing Interest

The authors declare that they have no known competing financial interests or personal relationships that could have appeared to influence the work reported in this paper.

Data Availability

Data will be made available on request.

Acknowledgments

This research was sponsored by the Faculty of Civil Engineering of Cracow University of Technology, Cracow, Poland.

References

[1] Rewers I. Cracking of Bent Concrete Beams Reinforced with High-strength Steel Sas 670/800, 293. Poland: Doctoral Thesis, Cracow Univeristy of Technology; 2022.
[2] Kahn LF, Mitchell AD. Shear Friction Tests with High-strength Concrete. ACI Structural Journal 2002;99:98–103.
[3] Fang Z, Tian X, Peng F. Flexural strength of prestressed Ultra-High-Performance concrete beams. 15 Eng Struct 2023;V. 279:115612. 12.
[4] Pozolo AM, Andrawes B. Transfer length in prestressed self-consolidating concrete box and I-girders. Acids Struct J 2011;V. 108(No 3):341–9.
[5] Myers JJ, Volz JS, Sells E, Porterfield K, Looney T, Tucker B, et al. Self-consolidating concrete (SCC) for infrastructure elements. TRyy1103 Roll: Mo Dep Transp, Final Rep 2012:36. TRyy1103.
[6] Okamura H, Ouchi M. Self-Compacting Concrete. J Adv Concr Technol 2000;1:5–15.
[7] Dyba M, Seruga A. Bond-slip relations in high performance concrete with plain steel bars. Acids Struct J 2024;V. 121(No 1):159–70.
[8] Seruga A, Dyba M. Bond strength between high-performance concrete and 7-mm non pretensioned plain steel wire.. accepted 05 Acids Struct J 2024. accepted 05.
[9] Dyba M. Influence of Technological Parameters on Concrete-steel Bond between High Performance Concrete and Prestressing Strands, Doctoral thesis, 340. Poland: Cracow University of Technology; 2014.
[10] Dybeł P. The Influence of the Composition and Properties of High Performance Concrete on the Bond Strength to Reinforcement Bars. Poland: Doctoral Thesis, Cracow Univeristy of Technology; 2012. p. 164–pp.
[11] Dybeł P, Furtak K. The effect of ribbed reinforcing bars location on their bond with high-performance concrete. Arch Civ Mech Eng 2015:1070–7.
[12] Kijania-Kontak M. Research of Bond between High Performance Concrete and High Strength Steel. Doctoral Thesis, Cracow University of Technology, Poland, 2018, 155 pp.
[13] Abrams D. Tests of Bond between Concrete and Steel, University of Illinois, Bulletin No. 71 Engineering Experimental Station. Urbana, IL: University of Illinois at Urbana-Champaign; 1913. p. 240–pp.
[14] Melo J, Rossetto T, Varum H. Experimental study of bond-slip in RC structural elements with plain bars. Mater Struct 2015;V.48(No.8):2367–81.
[15] Feldman LR, Bartlett FM. Bond strength variability in pullout specimens with plain reinforcement. ACI Struct J 2005;V.102(No.6):860–7.
[16] Feldman LR, Bartlett FM. Bond Stress along Plain Steel Reinforcing Bars in Pullout Specimens. ACI Struct J 2007;V.104(No.6):685–92.
[17] Ceb-fip Model Code 1990: Bulletin D'information No195, Comite Euro-international Du Beton, First Draft, Mars, 1990, Lausanne.
[18] CEB-FIP *Model Code 2010: Final draft*, march 2012, Volume 1, p.247 – 256, International Federation for Structural Concrete, Lausanne.
[19] Verderame GM, Ricci P, Carlo GD, Manfredi G. Cyclic bond behavior of plain bars. Part I: experimental investigation. Constr Build Mater 2009;23(12):3499–511.
[20] Verderame GM, Ricci P, Carlo GD, Manfredi G. Cyclic bond behavior of plain bars. Part II: analytical investigation. Constr Build Mater 2009;23(12):3512–22.
[21] Eligehausen R., Popov E.P., Bertero V.V. Local Bond Stress-slip Relationships of Deformed Bars under Generalized Excitations. Report no. UCB/EERC 83–23 1983, University of California at Berkeley.
[22] Magnusson J. Bond and Anchorage of Deformed Bars in High-strength Concrete. Chalmers University of Technology, Division of Concrete Structures, Licentiate Thesis, Publication 97:1, Göteborg, Sweden, 1997, 234 pp.
[23] Huang Z, Engström B, Magnusson J. Experimental Investigation of the Bond and Anchorage Behaviour of Deformed Bars in High-strength Concrete. Four International Symposium on the Utilization of high strength/ high performance concrete. Proceedings. Paris, France: Laboratories des Ponts et Chaussées; 1996. p. 1115–24.
[24] ACI Committee 226: Silica fume in concrete. ACI Mater J 1987;V. 84(No 2):158–66.
[25] Goldman A, Bentur A. Bond effects in high-strength silica-fume concretes. Acids Mater J 1989;V. 86(No 5):440–7.
[26] Gjørv OE, Menteiro PJM, Mehta PK. Effect of condensed silica fume on the steel-concrete bond. Acids Mater J 1990;V. 87(No 6):573–80.
[27] Okamura H, Ouchi M. Self-compacting high performance concrete. Prog Struct Eng Mater July 1998;V. 1(Iss. 4):378–83.
[28] PN-EN 12350–8:2012. Testing Fresh Concrete - Self-compacting Concrete. Part 8: Slump-flow test. Warsaw: PKN; 2012.
[29] ASTM C 1611. 2009. Standard Test Method for Slump Flow of Self-consolidating Concrete. West Conshohocken: American Society for Testing Materials (ASTM), 2009.
[30] CEB-FIP Bulletin 10: Bond of Reinforcement in Concrete. State of the art report. International Federation for Structural Concrete, Lausanne; 2000, 427 pp.
[31] CEB-FIPBulletin 72: Bond and Anchorage of Embedded Reinforcement: Background to the Fib Model Code for Concrete Structures *2010*. Technical Report. International Federation for Structural Concrete; 2014, 161 pp.
[32] CEB-FIPBulletin 106: *Advances on bond in concrete. State of the art report.* International Federation for Structural Concrete; 2022, 316 pp.
[33] Aci 408r-03: Bond and Development of Straight Reinforcing Bars in Tension. American Concrete Institute; 2003, 49 Pp.
[34] A1096/a1096m-15: Standard Test Method for Evaluating Bond of Individual Steel Wire, Indented Ora Plain, for Concrete Reinforcement. American Society for Testing Materials (Astm) International; 2015, 7 Pp.
[35] Seruga A. Bond Behaviour of Seven-wire Non-pretensioned Plain Strands Embedded in High-performance Concrete. 5th International Conference “Bond in Concrete” Stuttgart, Germany 25–27; 2022, Proceedings pp. 464–476.
[36] Seruga A, Dyba M. Bond Strength of High-performance Concrete to Seven-wire Tensioned Strands. 5th International Conference “Bond in Concrete” Stuttgart, Germany. Proceedings 2022:292–303.
[37] Seruga A., Dyba M. Transmission Length of Prestressing 7ϕ5 Mm Strand in Axially Prestressed High-performance Concrete Members. 5th International Conference “Bond in Concrete” Stuttgart, Germany 25–27 July 2022, Proceedings pp. 567–578.
[38] Wang J, Yang L, Yang J. Bond behavior of epoxy-coated reinforcing bars with seawater sea-sand concrete. Acids Struct J July 2020;V.117(No.4):193–208.
[39] Diab A, Elyamany H, Felfel M, Ashy H. Bond behavior and assessment of design ultimate bond stress of normal and high strength concrete. Alex Eng J 2014;V.53 (No.2):355–71. https://doi.org/10.1016/j.aej.2014.03.012.
[40] Xiao J., Long X., Ye M., Jiang H., Liu L., Zhai K. Experimental Study of Bond Behavior between Rebar and Pva-engineered Cementitious Composite (Ecc) Using Pull-out Tests. Frontiers in Materials, V.8., art. 633404, 15 pp. 10.3389/fmats.2021.633404.